

# RSC Advances



This is an *Accepted Manuscript*, which has been through the Royal Society of Chemistry peer review process and has been accepted for publication.

*Accepted Manuscripts* are published online shortly after acceptance, before technical editing, formatting and proof reading. Using this free service, authors can make their results available to the community, in citable form, before we publish the edited article. This *Accepted Manuscript* will be replaced by the edited, formatted and paginated article as soon as this is available.

You can find more information about *Accepted Manuscripts* in the [Information for Authors](#).

Please note that technical editing may introduce minor changes to the text and/or graphics, which may alter content. The journal's standard [Terms & Conditions](#) and the [Ethical guidelines](#) still apply. In no event shall the Royal Society of Chemistry be held responsible for any errors or omissions in this *Accepted Manuscript* or any consequences arising from the use of any information it contains.

# One-step Hydrothermal Synthesis and Optical Properties of PEG-passivated Nitrogen-doped Carbon Dots†

Ben-Xing Zhang,<sup>a</sup> Gang-Yi Zhang,<sup>a</sup> Hui Gao,<sup>\*a</sup> Shao-Hui Wu,<sup>a</sup> Jian-Hua Chen,<sup>a</sup> and Xiao-Long Li<sup>b</sup>

<sup>a</sup> School of Physical Science and Technology, Key Laboratory for Magnetism and Magnetic Materials of Ministry of Education, Lanzhou University, Lanzhou 730000, P. R. China

E-mail: hope@lzu.edu.cn; Fax: +81 931 8913554; Tel: +81 931 8912772

<sup>b</sup> Shanghai Synchrotron Radiation Facility, Shanghai Institute of Applied Physics, Chinese Academy of Sciences, Shanghai 201204, P. R. China

\* Corresponding author.

† Electronic Supplementary Information (ESI) available.

## Abstract

Strong fluorescent polyethylene glycol passivated nitrogen-doped carbon dots (P-NCDs) were prepared through a one-step facile hydrothermal process using glutamic acid as the precursor. The passivated nitrogen-doped carbon dots with the average size of 6.5 nm showed strong blue luminescence excited with ultraviolet light. Excitation wavelength dependent photoluminescence was observed in the obtained P-NCDs, and the relationship between the excitation and emission wavelength could be formulated as a linear function. The P-NCDs exhibit noticeable enhancement of photoluminescence after the passivation and the quantum yield was as high as 18.7%. The P-NCDs also exhibited the luminescence resistance to heavy metal ions to some extent. The excellent comprehensive properties enable the P-NCDs to have potential applications in detecting the polluted environment and other bio-imaging fields.

## 1 Introduction

Carbon dots (CDs), the fluorescence carbon nanoparticles, have drawn tremendous attention since Xu *et al.* reported them firstly in 2004.<sup>1</sup> Compared with traditional quantum dots, CDs possess the virtues of abundant precursors, excellent solubility in various kinds of solvent, preferable biocompatibility, and exceptional resistance to photobleaching.<sup>2</sup> Therefore, CDs have huge potential applications in a wide range of fields: ion detection,<sup>3</sup> pH sensor,<sup>4</sup> bioimaging,<sup>5</sup> oxygen (O) reduction reaction,<sup>6</sup> and drug delivery<sup>7</sup>, to name a few. Various strategies for preparing and doping of CDs were mainly divided into two groups: the bottom-up methods (arc discharge,<sup>1</sup> laser ablation,<sup>8</sup> electrochemical synthesis<sup>9</sup> *et al.*) and the top-down methods (carbohydrate-heating,<sup>10</sup> combustion routes,<sup>1</sup> ultrasonic treatment<sup>12</sup> *et al.*). Compared with the bottom-up methods, the top-down approaches inevitably suffer from low yield, complicated process, and severe synthesis conditions.

To date, heteroatoms such as nitrogen (N),<sup>13</sup> sulfur (S),<sup>14</sup> and boron (B)<sup>15</sup> have been incorporated into the framework of the carbon nanoparticles successfully. It's especially watchable that conspicuous progresses have been made on N doped CDs (NCDs). N-doping has been proved to modify the electron density and improve the chemical activities and photic properties.<sup>11</sup> Similar radius between the atoms of C and N (the radius of C: 0.77 Å, N: 0.75 Å) facilitates N atoms to be incorporated into the C matrix. Furthermore, strong covalent bond between C and N brings about long-term stability in the NCDs. Glutamic acid (GA) is the benign source of C and N because of its cheapness and abundance. Recently,

glutamic acid (GA) was used as the precursor for synthesizing nitrogen doped carbon nanoparticles by heating process.<sup>16,17</sup> GA is a green and very cheap amino acid, which plays an important role in the metabolism of human body. And it contains abundant functional groups such as carboxylic acid and amino, which would react effectively in the formation of NCDs. However, it is hard to control the heating process accurately and this would affect the homogeneity of the final products. In addition to that, the prepared CDs only handled with doping process possess the insufficient luminescence.<sup>18</sup> Sun's group<sup>19</sup> demonstrated that the surface passivation makes a significant contribution to bright PL and the passivated defects are crucial to excitation energy traps. Up to now, polyethylene glycol (PEG),<sup>15</sup> polyethylenimine,<sup>16</sup> ethylenediamine,<sup>17</sup> 1-hexadecylamine<sup>18</sup> *et al.* have been confirmed to act as the agent of passivators. Normally, the passivation process was another independent procedure after the preparation of NCDs,<sup>19, 20, 21</sup>

In our research, we adopted a facile one-step hydrothermal method of preparing PEG<sub>6000</sub>-passivation NCDs (P-NCDs) using GA as the precursor. The choose of PEG<sub>6000</sub> is due to its high molecular weight, which would contain its polymeric structure under hydrothermal condition for further passivated the NCDs. Besides that, PEG has good water solubility and should be beneficial to biocompatibility. The results indicated that the existence of carbonization and amidation in the reaction process. The obtained P-NCDs exhibit significant enhancement in the brightness of PL (the quantum efficiency of *ca.* 18.7%) when compared with passivation-free NCDs as well as the resistance to heavy metal ions.

## 2 Experimental

GA, PEG<sub>6000</sub>, and other chemicals were purchased from Sinopharm Chemical Reagent Co., Ltd. All chemicals were analytical agent without further note and used as received. Ultra pure water used in the whole experiment holds the resistivity greater than 18.1 MΩ\*cm.

### 2.1 Preparation of samples

In a typical procedure, 0.5 g GA and 0.9 g PEG were added into 20 ml ultra pure water. The mixture was stirred drastically to form a homogeneous solution and then transferred into a teflon-lined autoclave. The sealed pot was maintained at 180 °C for 9 h in an electric oven. After cooling to room temperature, the obtained yellow solution was drying in a vacuum to obtain powdered P-NCDs. For comparison, passivation-free NCDs were also prepared under the similar conditions.

PbCl<sub>2</sub>, Cd(NO<sub>3</sub>)<sub>2</sub>·4H<sub>2</sub>O, and CuCl<sub>2</sub>·2H<sub>2</sub>O were selected as the sources of heavy metal ions and each ion solution was conected to the concentration of 0.01 mol L<sup>-1</sup>. In all ion batches, 0.5 ml of metal ion solution was blended into 10 ml P-NCDs solution to form a homogeneous solution, respectively. The blank batch was diluted with 0.5 ml ultra pure water too. The corresponding PL spectra were recorded at the excitation of 350 nm after 0.5 h.

### 2.2 Apparatus

Ultra pure water was gained from Millipore Elix 5 UV and Milli-Q Gradient Ultra-pure Water System. The transmission electron microscopy (TEM) and high resolution TEM observation was made on a F-30 S-TWIN electron microscope (Tecnai G2, FEI Company) at 20 °C. The size distribution and histogram were completed through the software of Nano Measurer 1.2. X-ray photoelectron spectra (XPS, PHI-5702, Physical Electronics) were obtained using a monochromated Al-Kα irradiation. The Fourier transform infrared (FT-IR) spectra were registered between 275 and 4000 cm<sup>-1</sup> on a FT-IR spectrometer (Nicolet

NEXUS 670) using KBr pellets. The PL spectra and fluorescence emission spectra were recorded on an FLS-920T fluorescence spectrophotometer and a HORIBA JOBIN YVON Fluorolog-3 Spectrofluorometer system at 16 °C, respectively. The quantum yield was calculated using quinine sulfate as the reference. UV-Vis absorption spectra were performed on a Perkin Elmer 950 spectrophotometer. Raman scattering spectra were obtained using a Renishaw InVia Raman microscope with 532 nm line of an Ar ion laser as an excitation source. The decay curve was recorded on a PR305 phosphorophotometer. Without further statement, all the measurements were performed at room temperature.

### 3 Results and discussion

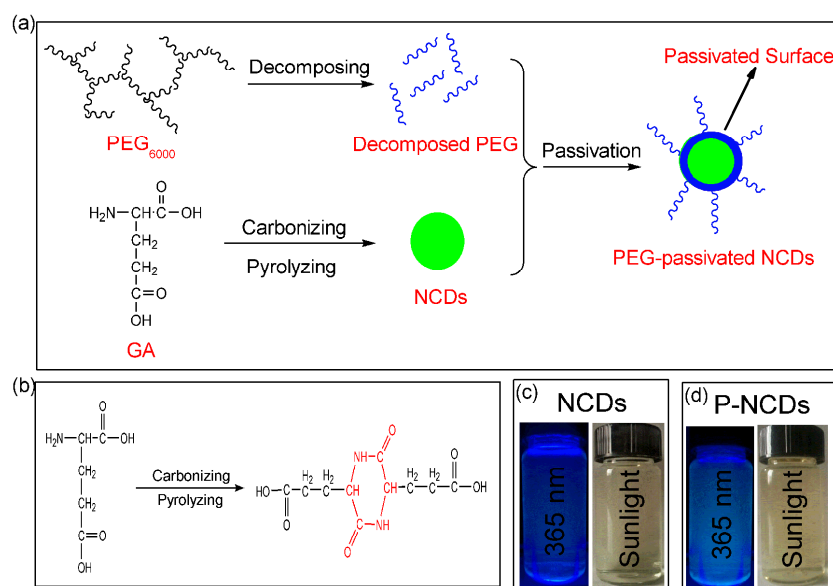


Fig. 1 (a) Schematic formation of P-NCDs. (b) Details about the preliminary amidation of GA. The digital photos of NCDs (c) and P-NCDs (d) under sunlight and 365 nm, respectively.

In this study, we synthesized P-NCDs through a facile and efficient process. The schematic formation of P-NCDs was shown in Fig. 1a. Under the hydrothermal condition, GA was carbonized and pyrolyzed to form NCDs, and the long chain of PEG<sub>6000</sub> was partially broken due to its high molecular weight. After the reaction, the obtained NCDs were passivated with the decomposed PEG<sub>6000</sub> to form the P-NCDs. Various reactions could be happened at the same time. Based on the molecular structure of GA, the XPS and IR analyses, the carbonization and amidation (such as forming the hexatomic ring and lactam) would occur in the hydrothermal reactions. The preliminary possible reaction for forming the hexatomic ring was provided in the Fig. 1b. Fig. 1c and 1d showed the digital photos of the pristine NCDs and P-NCDs under sunlight and 365 nm, respectively. Both of the carbon dots were well-dispersed in the water. Under the sunlight, the brown color of P-NCDs was deeper than that of NCDs. And the brightness of NCDs was higher after the passivation.

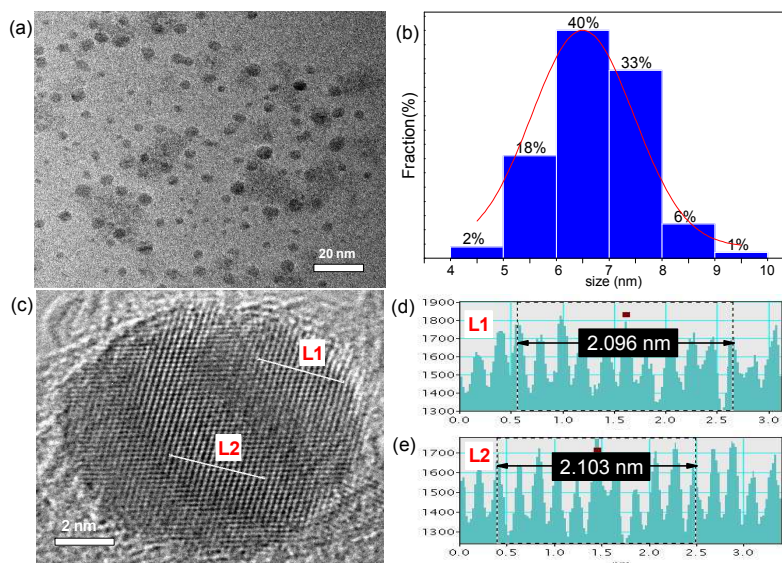


Fig. 2 (a) TEM image of P-NCDs. (b) Size distribution and histogram. (c) High resolution TEM image of P-NCDs. High profile along corresponding line L1 (d) and L2 (e).

The as prepared P-NCDs were polydisperse and the mean diameter was 6.5 nm, as shown in Fig. 2a and b. Size distribution analysis (Gaussian curve) demonstrated that the range of size was  $7.0 \pm 3.0$  nm. Although the polydisperse was an inevitable problem when the teflon-lined autoclave cooled to room temperature gradually and slowly, 90% of particles were included in a narrow range. The high resolution TEM image of P-NCDs revealed the distinct lattice structure in Fig. 2c, indicating their highly crystalline. The lattice space of 0.2096 nm and 0.2103 nm were calculated from the detailed line profile of L1 and L2 (Fig. 2d and 2e), respectively. The average distance for P-NCDs was 0.21 nm, in accordance with the previous reports, which was attributed to the (100) of graphene (in-plane).<sup>14,22</sup> In order to investigate the size effect of passivation, we also compared the TEM images of P-NCDs and NCDs (Fig. S1, ESI†) and found that there was a slight increasing for average size of dots (from 5.9 nm to 6.5 nm) after passivation, which were due to the coverage of PEG<sub>6000</sub> on the surface of NCDs.

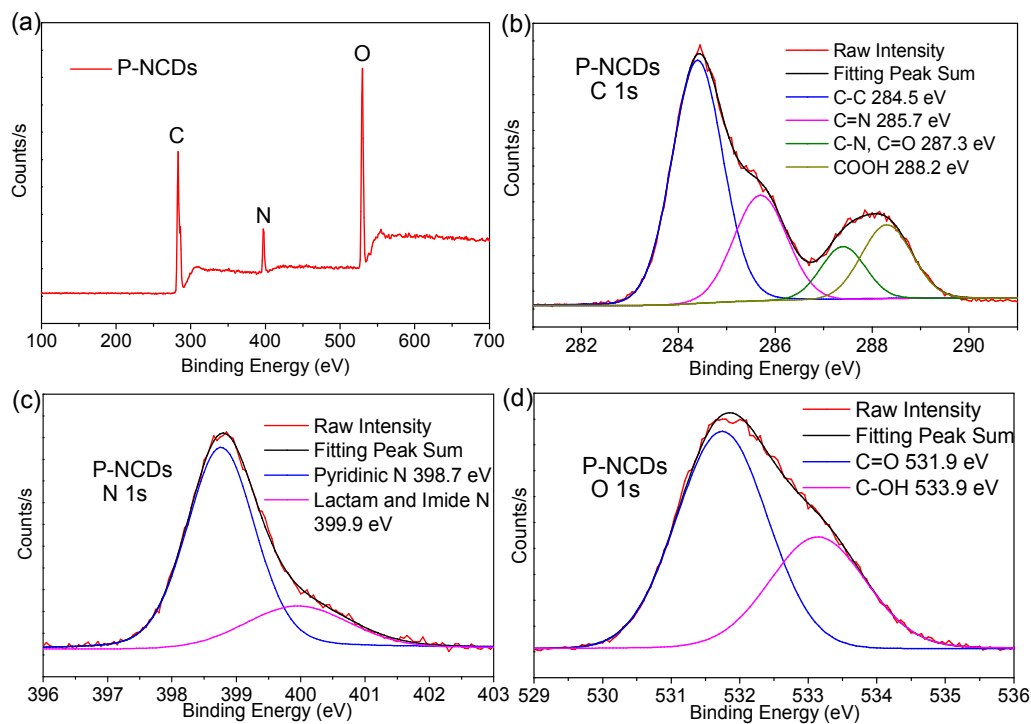


Fig. 3 (a) The full scan XPS of P-NCDS. High resolution XPS of C 1s (b), N 1s (c) and O 1s (d).

XPS could provide us the composition of elements and their chemical state. The atoms of C, N, and O in P-NCDS were detected at the peaks of *ca.* 284 eV, 400 eV, and 533 eV, respectively, as shown in Fig. 3a. The composition of P-NCDS was calculated to 42.4 at.% of C, 9.3 at.% of N, and 48.3 at.% of O according to the full scan spectra. A high resolution XPS for C1s, N1s and O1s were given in Fig. 3b, 3c and 3d. As shown in the fine C spectrum, distinct peaks at 284.5 eV, 285.7 eV, 287.3 eV, and 288.2 eV were attributed to the bonds of graphite-like  $sp^2$  C, C=N, C-N (overlapped with C=O) and COOH, respectively.<sup>23-25</sup> Thus, the N doping of carbon dots could be confirmed by the bonds between C and N. The high-resolution of N spectrum could be divided into two main peaks: 398.7 eV of pyridinic N and 399.9 eV of lactam and imide N.<sup>26</sup> And it was proposed that amino-groups would react with carboxylic acid groups and form the lactam N or imide N in the structure of P-NCDS, which was in agreement with our possible reaction process (Fig. 1b). High resolution image indicated that O atoms mainly presented in two groups: C=O and C-OH,<sup>27</sup> in line with the conclusions from the analysis of C spectra. FT-IR spectra of P-NCDS, GA and PEG<sub>6000</sub> were shown in Fig. S2 (ESI<sup>†</sup>). Comparing curve P-NCDS with others, the stretching vibrations of N-H were observed at *ca.* 3300  $cm^{-1}$ . Besides that, the strong peaks from 1630 to 1740  $cm^{-1}$  resulted from the carboxylic acid C=O and amide C=O stretches in the P-NCDS. C=C stretching was formed by the appearance of 1435  $cm^{-1}$ , indicating the carbonization of GA into the graphite-like carbon dots structure.<sup>28</sup> These data are in well agreement with XPS results. We examined the Raman spectra of the samples (Fig. S3, ESI<sup>†</sup>), and the fluorescence background of Raman spectra was removed through an intelligent algorithm.<sup>29</sup> The ratio of disorder (D) band and graphite (G) band represented the degree of disorder in C material and the level of the defect amount. As shown in Fig. S3, the ratio of  $I_D/I_G$  was higher after the passivation, implying more defects introduced into the NCDS.

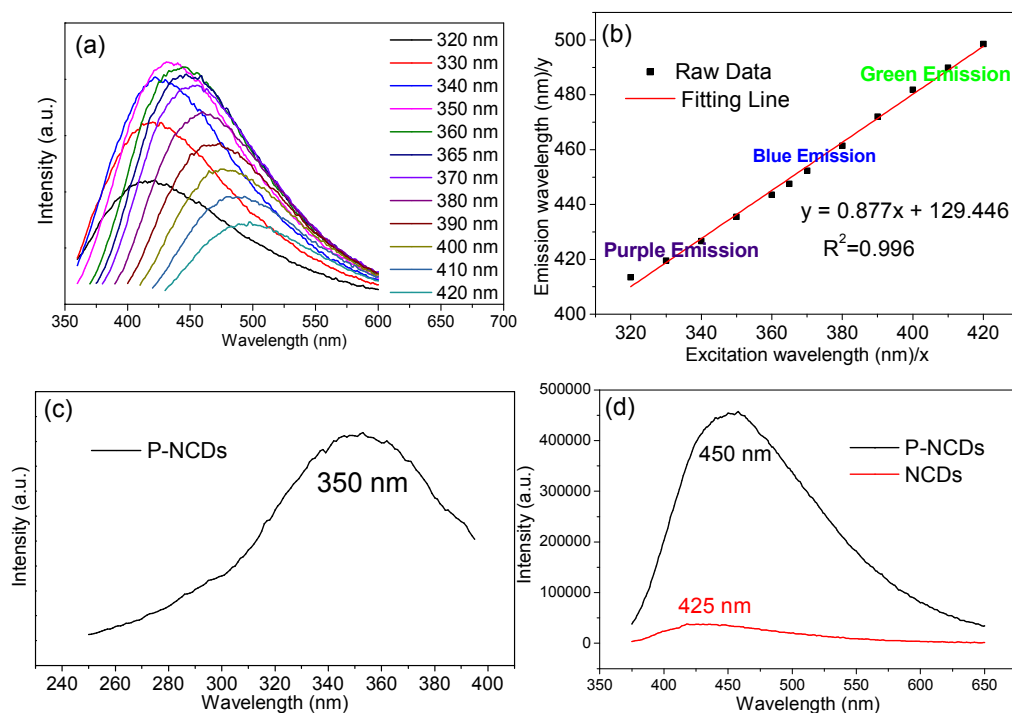


Fig. 4 (a) PL spectra of P-NCDs under a series of excitation wavelength. (b) The function relationship between the emission and excitation wavelength. (c) PL excitation spectra of P-NCDs detected under 435 nm. (d) PL intensity of P-NCDs and NCDs excited at 350 nm.

Excitation wavelength dependent PL were observed in the P-NCDs (Fig. 4a and 4b). Emission wavelength shifted from 415 nm (purple) to 500 nm (green) when the excitation wavelength escalated from 320 nm to 420 nm with the strongest emission intensity at 435 nm. The phenomena could be due to the emissions from different size NCDs as well as the different emissive sites on each passivated NCDs.<sup>30</sup> Interestingly, the relationship between the excitation and emission wavelength could be formulated as the linear fitting function:  $y = a \cdot x + b$ . Using this precise function, we could reckon the excitation wavelength in order to gain specific color in applications. In addition to that, it was observed great enhancement of PL intensity in P-NCDs compared with passivation-free NCDs (Fig. 4d). Previous literature<sup>19</sup> noted that this phenomenon was put down to the changes of the surface state. Passivated defects were introduced through the passivation process, which would bring more excitation energy traps. Therefore, more photons of excitation beam could be captured and transformed into emission irradiation with the Stokes shift of *ca.* 90 nm. At the same time, it was also a noteworthy fact that there was a slight increase (from 425 nm to 450 nm) of the emission wavelength when PEG was adhered on the surface. According to the results in the TEM data, the passivation process enlarged the size of P-NCDs. The larger size of fluorescent nanodots could conduce the red shift of the emission peak.<sup>2</sup> Therefore, it is reasonable that the size effect of passivation accounts for this slight shift. In addition, the quantum yield of P-NCDs was calculated to *ca.* 18.7% (under 350 nm) using quinine sulfate as the reference, and the lifetime curve was complying with tri-exponential decay with the lifetime of 5.5 ns (Fig. S4 ESI†). In Fig. 4c, a wide peak around 350 nm was observed in the PL excitation (PLE) spectra, which conforms to the conclusion that the strongest emission intensity is obtained with an excitation wavelength of 350 nm. Characteristic peaks are illustrated in UV-Vis absorption curve (Fig. S5, ESI†). Apart from the edge absorption, peaks at *ca.* 230 nm, 280 nm, and 325 nm are assigned to  $\pi \rightarrow \pi^*$  of conjugated diene,  $\pi \rightarrow \pi^*$  of C=N, and  $n \rightarrow \pi^*$  of C=O,

respectively.<sup>31</sup> The energy levels are displayed in Fig. S6 (ESI†). The introduction of N atoms brought about the new energy level. This N energy level was regarded as “bridge” which is essential to the absorption at 280 nm.<sup>14</sup>

Interestingly, as shown in Fig.5 the luminescence of P-NCDs exhibited resistance to heavy metal ions ( $\text{Pb}^{2+}$ ,  $\text{Cd}^{3+}$  and  $\text{Cu}^{2+}$ ) to some extent. Previous studies<sup>3</sup> indicated that the presence of some heavy metal ions could lead to the luminescence quenching of CDs and the probable mechanism was the formation of complexes between ions and hydroxyl groups. And in our research, the P-NCDs exhibited less effectively quenching properties for the heavy metal ions compared with that of CDs, which would be related to the hydrothermal process. As mentioned before, the hydroxyl groups from  $-\text{COOH}$  could react mostly with the  $-\text{NH}_2$  groups. When introducing the heavy ions into the P-NCDs, the possibility of the complexing reactions would decrease and lead to the above surprising phenomenon.

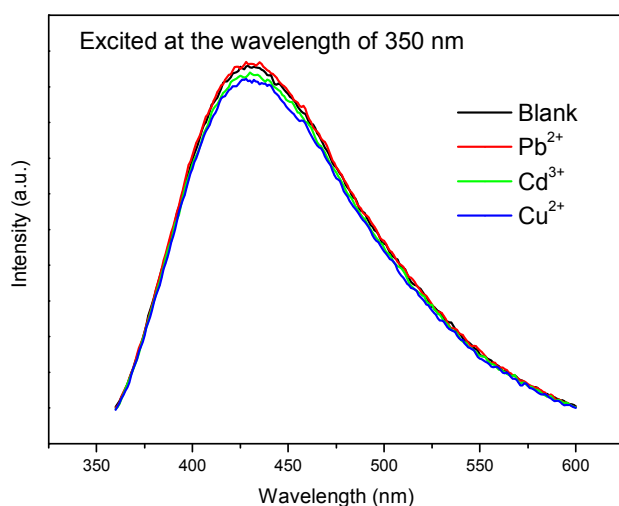


Fig. 5 The emission spectrum of P-NCDs mixing with heavy metal ions after 0.5 h

In brief, we have developed a one-step facile method for preparing P-NCDs. The obtained product exhibited brighter photoluminescence than those without passivated. The carbonization and amidation would occur in the complex reactions. Excitation wavelength dependent PL was observed and the relationship between excitation and the corresponding emission wavelength could be formulated as the linear fitting function. In addition, the luminescence of P-NCDs exhibit resistance to heavy metal ions to some extent.

## 5 Acknowledgements

This work was financially supported by the Natural Science Foundation of Gansu Province, China (Grant No. 1208RJYA005), the National Science Foundation of China (51402140, 11205235) and the National Basic Research Program of China (973 program) (2010CB934501).

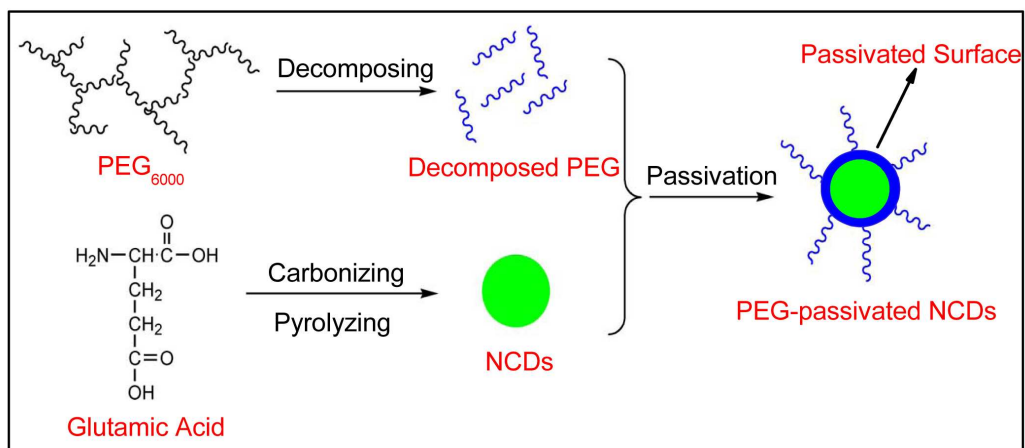
## 6 References

1. X. Xu, R. Ray, Y. Gu, H. J. Ploehn, L. Gearheart, K. Raker and W. A. Scrivens, *Journal of the American*

- Chemical Society*, 2004, 126, 12736-12737.
2. S. N. Baker and G. A. Baker, *Angewandte Chemie International Edition*, 2010, 49, 6726-6744.
  3. Y.-L. Zhang, L. Wang, H.-C. Zhang, Y. Liu, H.-Y. Wang, Z.-H. Kang and S.-T. Lee, *RSC Advances*, 2013, 3, 3733.
  4. Y. Mao, Y. Bao, L. Yan, G. Li, F. Li, D. Han, X. Zhang and L. Niu, *RSC Advances*, 2013, 3, 5475-5482.
  5. P. G. Luo, S. Sahu, S.-T. Yang, S. K. Sonkar, J. Wang, H. Wang, G. E. LeCroy, L. Cao and Y.-P. Sun, *Journal of Materials Chemistry B*, 2013, 1, 2116-2127.
  6. S. Yang, X. Feng, X. Wang and K. Müllen, *Angewandte Chemie International Edition*, 2011, 50, 5339-5343.
  7. Q. Wang, X. Huang, Y. Long, X. Wang, H. Zhang, R. Zhu, L. Liang, P. Teng and H. Zheng, *Carbon*, 2013, 59, 192-199.
  8. L. Cao, X. Wang, M. J. Meziani, F. Lu, H. Wang, P. G. Luo, Y. Lin, B. A. Harruff, L. M. Veca, D. Murray, S.-Y. Xie and Y.-P. Sun, *Journal of the American Chemical Society*, 2007, 129, 11318-11319.
  9. J. Zhou, C. Booker, R. Li, X. Zhou, T.-K. Sham, X. Sun and Z. Ding, *Journal of the American Chemical Society*, 2007, 129, 744-745.
  10. B. De and N. Karak, *RSC Advances*, 2013, 3, 8286-8290.
  11. H. Liu, T. Ye and C. Mao, *Angewandte Chemie International Edition*, 2007, 46, 6473-6475.
  12. Z. Ma, H. Ming, H. Huang, Y. Liu and Z. H. Kang, *New J Chem*, 2012, 36, 861-864.
  13. Z. Yang, M. H. Xu, Y. Liu, F. J. He, F. Gao, Y. J. Su, H. Wei and Y. F. Zhang, *Nanoscale*, 2014, 6, 1890-1895.
  14. B.-X. Zhang, H. Gao and X.-L. Li, *New J Chem*, 2014, 38, 4615-4621.
  15. S. Dey, A. Govindaraj, K. Biswas and C. N. R. Rao, *Chemical Physics Letters*, 2014, 595-596, 203-208.
  16. J. Niu, H. Gao, L. Wang, S. Xin, G. Zhang, Q. Wang, L. Guo, W. Liu, X. Gao and Y. Wang, *New J Chem*, 2014, 38, 1522-1527.
  17. X. Wu, F. Tian, W. Wang, J. Chen, M. Wu, J. X. Zhao, *J Mater Chem C*, 2013, 1, 4676-4684.
  18. Z. Lin, W. Xue, H. Chen and J.-M. Lin, *Chemical communications*, 2012, 48, 1051-1053.
  19. Y.-P. Sun, B. Zhou, Y. Lin, W. Wang, K. A. S. Fernando, P. Pathak, M. J. Meziani, B. A. Harruff, X. Wang, H. Wang, P. G. Luo, H. Yang, M. E. Kose, B. Chen, L. M. Veca and S.-Y. Xie, *Journal of the American Chemical Society*, 2006, 128, 7756-7757.
  20. C. Liu, P. Zhang, X. Zhai, F. Tian, W. Li, J. Yang, Y. Liu, H. Wang, W. Wang and W. Liu, *Biomaterials*, 2012, 33, 3604-3613.
  21. H. Peng and J. Travas-Sejdic, *Chemistry of Materials*, 2009, 21, 5563-5565.
  22. Y. Dong, H. Pang, H. B. Yang, C. Guo, J. Shao, Y. Chi, C. M. Li and T. Yu, *Angewandte Chemie*, 2013, 52, 7800-7804.
  23. Y. Li, Y. Zhao, H. Cheng, Y. Hu, G. Shi, L. Dai and L. Qu, *Journal of the American Chemical Society*, 2012, 134, 15-18.
  24. Q. Liu, B. Guo, Z. Rao, B. Zhang and J. R. Gong, *Nano letters*, 2013, 13, 2436-2441.
  25. R. J. J. Jansen and H. Vanbeekum, *Carbon*, 1995, 33, 1021-1027.
  26. Y. Chen, J. Wang, H. Liu, M. N. Banis, R. Li, X. Sun, T.-K. Sham, S. Ye and S. Knights, *The Journal of Physical Chemistry C*, 2011, 115, 3769-3776.
  27. H. Gao, L. Song, W. Guo, L. Huang, D. Yang, F. Wang, Y. Zuo, X. Fan, Z. Liu, W. Gao, R. Vajtai, K. Hackenberg and P. M. Ajayan, *Carbon*, 2012, 50, 4476-4482.
  28. D. Sun, R. Ban, P. H. Zhang, G. H. Wu, J. R. Zhang and J. J. Zhu, *Carbon*, 2013, 64, 424-434.
  29. Z.-M. Zhang, S. Chen, Y.-Z. Liang, Z.-X. Liu, Q.-M. Zhang, L.-X. Ding, F. Ye and H. Zhou, *Journal of*

- Raman Spectroscopy*, 2009, 41, 659-669.
30. P. Russo, A. M. Hu, G. Compagnini, W. W. Duley and N. Y. Zhou, *Nanoscale*, 2014, 6, 2381-2389.
31. L. B. Tang, R. B. Ji, X. M. Li, K. S. Teng and S. P. Lau, *J Mater Chem C*, 2013, 1, 4908-4915.

## One-step Hydrothermal Synthesis and Optical Properties of PEG-passivated Nitrogen-doped Carbon Dots



PEG-passivation enhanced the luminescence intensity of nitrogen-doped carbon dots markedly